PHYSICAL REVIEW E VOLUME 56, NUMBER 5 NOVEMBER 1997

Symmetry-breaking instabilities of spatial parametric solitons

Alfredo De Rossi and Stefano Trillo
Fondazione Ugo Bordoni, Via B. Castiglione 59, 00142 Roma, Italy

Alexander V. Buryak and Yuri S. Kivshar
Australian Photonics Cooperative Research Centre, Research School of Physical Sciences and Engineering, Optical Sciences Centre, The Australian National University, Canberra, Australian Capital Territory 0200, Australia

(Received 26 June 1997)

We investigate the symmetry-breaking (temporal or transverse) instabilities of (1+1)- and (2+1)-dimensional two-wave parametric solitons sustained through the interplay of diffraction and second-harmonic generation. [S1063-651X(97)50911-1]

PACS number(s): 42.65.Tg, 42.65.Sf, 42.65.Ky

For three decades optical spatial solitons confined in the transverse plane were commonly believed to be a prerogative of media with cubiclike nonlinearities [1]. A remarkable exception is the work carried out in Ref. [2], where the possibility to achieve diffraction-free propagation via three-photon interactions in quadratic media (henceforth, parametric solitons) was first pointed out. The field of quadratic solitons has acquired importance only recently [3], also stimulated by experiments in second-harmonic generation (SHG) in bulk media (2+1 dimensions) and planar waveguides (1+1 dimensions) [4].

Since the parametric solitons are strictly speaking solitary waves (the model equations are not integrable), a crucial issue is their stability. Two main types of instabilities can be distinguished: (i) *longitudinal* instability against perturbations that share the soliton symmetry [5]; (ii) *symmetry-breaking* instabilities (reminiscent of modulational instabilities of plane-waves [6]), that take place whenever the solitons are embedded in a higher dimensional ''space'' with respect to the subspace in which they are localized [7,8]. For the former type of problem, stability criteria have been recently developed [5], through asymptotic techniques [9]: both (1+1)- and (2+1)-dimensional parametric solitons are stable in the largest portion of their existence domain in the parameter space. Moreover, the global stability (no collapse) of (2+1)- and (3+1)-dimensional parametric solitons and bullets is supported by the Liapunov-type stability analysis [10]. Conversely, the symmetry breaking of parametric solitons is still an open issue, even though the problem has been widely studied for cubic media [7]. Here we investigate the stability of the whole one-parameter families of ground-state planar SHG solitons. We anticipate that the development of the instability leads either to the formation of lattices of higher dimensional solitons, or to the complete disintegration (radiative decay) of the soliton. The transverse instability of soliton stripes belongs to the former case, whereas the dynamics of temporal instabilities of both (1+1)- and (2+1)-dimensional solitons depends on the dispersive regime. Our results are of great importance for recent experiments in transverse pattern formation occurring via SHG [11,12]. In particular, the filamentation of beams with strongly elliptical cross sections (i.e., pseudostripe) was already observed [11], using nonsoliton input conditions (i.e., SHG from the fundamental). The plane-wave approach developed in Ref. [11] accounts for the dynamics of SHG, whereas the effect of confinement (along the ellipse minor axis) was not analyzed. Here we focus on the latter aspect, and show results which serve as a guideline for ongoing SHG experiments. We make use of the usual model for SHG [3], governing the interaction of the field envelopes u_1 at fundamental, and u_2 at second-harmonic frequency

$$-i\frac{\partial u_1}{\partial Z}=\frac{\delta H}{\delta u_1^*}=\frac{1}{2}\nabla^2 u_1-\frac{\gamma_1}{2}\frac{\partial^2 u_1}{\partial T^2}+u_2u_1^*,$$
$$-i\frac{\partial u_2}{\partial Z}=\frac{\delta H}{\delta u_2^*}=\frac{1}{2\sigma}\nabla^2 u_2-\frac{\gamma_2}{2}\frac{\partial^2 u_2}{\partial T^2}+\delta k\ u_2+\frac{u_1^2}{2}, \qquad (1)$$

where $\nabla^2=\partial_X^2+\partial_Y^2$, with $X,Y\equiv(x,y)/r_0$ transverse coordinates in units of the beam width r_0, $Z\equiv z/z_d$ is the propagation distance in units of diffraction length $z_d=k_1r_0^2$, $\delta k\equiv\Delta k z_d=(k_2-2k_1)k_1r_0^2$ is the phase mismatch, $\sigma\equiv k_2/k_1$, $T\equiv(z_d|k_1''|)^{-1/2}(t-z/V)$ is the normalized time in a frame traveling at common group velocity V, $k_{1,2}''\equiv\partial^2k/\partial\omega^2|_{\omega_0,2\omega_0}$, $\gamma_1=\mathrm{sgn}(k_1'')$, and $\gamma_2=\mathrm{sgn}(k_2'')|k_2''/k_1''|$. Furthermore $u_1\equiv\sqrt{2}z_d\chi E_1$, $u_2\equiv z_d\chi E_2\exp(i\Delta kZ)$, where $|E_{1,2}|^2$ are the intensities, and $\chi\equiv(\omega_0/c)[2/(c\epsilon_0 n_{\omega_0}^2 n_{2\omega_0})]^{1/2}d_{eff}$. Two conserved quantities of Eqs. (1) that play an important role in our analysis are $H=\int_{-\infty}^{+\infty}H_d\ d\vec{S}$, $N=\int_{-\infty}^{+\infty}N_d\ d\vec{S}$, where $\vec{S}=(X,Y,T)$, $H_d=\delta k|u_2|^2+\frac{1}{2}(u_1^2u_2^*+\text{c.c.}-|\nabla^2u_1|^2-|\nabla^2u_2|^2/\sigma+\gamma_1|u_{1T}|^2+\gamma_2|u_{2T}|^2)$ and $N_d=|u_1|^2+2|u_2|^2$ are Hamiltonian and photon flux density, respectively. Our conclusions remain qualitatively valid when a weak spatial or temporal walk-off term in Eqs. (1) contribute to break the soliton symmetry.

For cw light (i.e., $\partial/\partial T=0$), Eqs. (1) possess two types of two-color bright solitary solutions trapped in the transverse plane: (1) soliton stripes confined along one dimension, say X; (2) solitons with cylindrical symmetry. Both constitute a one-parameter family of bounded solutions $u_1\equiv u_{1s}=(\mu/\sqrt{\sigma})\ x_1(\sqrt{\mu}\rho)\ \exp(i\mu Z)$ and $u_2\equiv u_{2s}=\mu\ x_2(\sqrt{\mu}\rho)\ \exp(i2\mu Z)$ (with μ positive for spatial bright solitons [3]), $x_{1,2}$ being (real) separatrix trajectories of the equivalent mechanical system $x''_{1,2}+(s/\rho)x'_{1,2}=-\partial V/\partial x_{1,2}$, where the potential $V(x_1,x_2)=-x_1^2-\alpha x_2^2+x_2x_1^2$, and the prime stands for $d/d\rho$, with $\rho=\sqrt{\mu}X$, $s=0$ for stripes (1) or $\rho=\sqrt{\mu(X^2+Y^2)}$, $s=1$ for cylindrical solitons (2). Note that the normalized soliton profiles are determined only by the normalized parameter $\alpha\equiv\sigma(2-\delta k/\mu)$, whereas the stability depends on both σ and α [5]. We investigate symmetry-breaking instability of the parametric solitons, looking for exponentially growing perturbations $a_{1,2}$ of the fields $u_{1s,2s}$ in the form $u_1=\mu/\sqrt{\sigma}[x_1(\rho)+a_1]\exp(i\mu Z)$, $u_2=\mu[x_2(\rho)+a_2]\exp(i2\mu Z)$. From Eqs. (1) we obtain the following linear equations for the perturbations:

$$-i\frac{da_1}{d\zeta}=\frac{1}{2}\left(r_1\Delta-\beta_1\frac{\partial^2}{\partial\tau^2}\right)a_1-a_1+x_1a_2+x_2a_1^*,$$

$$-i\sigma\frac{da_1}{d\zeta}=\frac{1}{2}\left(r_2\Delta-\beta_2\frac{\partial^2}{\partial\tau^2}\right)a_2-\alpha a_2+x_1a_1, \tag{2}$$

where $r_1=r_2\equiv\mathrm{sgn}(\mu)=1$, $\beta_1\equiv\mathrm{sgn}(\mu)\gamma_1$, $\beta_2\equiv\mathrm{sgn}(\mu)\sigma\gamma_2$, and we introduced the variable $\zeta=\mu Z$ and the transverse Laplacian $\Delta=\partial_\xi^2+\partial_\eta^2$, with $(\xi,\eta,\tau)\equiv\sqrt{|\mu|}(X,Y,T)$. We consider periodic perturbations, and single out three different cases of physical relevance: (a) $a_{1,2}=[\epsilon_{r1,2}(\xi)+i\epsilon_{i1,2}(\xi)]\cos(\Omega\eta)$ with $\beta_{1,2}=0$ corresponding to a transverse instability of a parametric soliton stripe in a bulk medium, usually observable in quasi-cw experiments [11]; (b) $a_{1,2}=[\epsilon_{r1,2}(\xi)+i\epsilon_{i1,2}(\xi)]\cos(\Omega\tau)$ with $\partial_\eta^2\to 0$, describing temporal instabilities of one-dimensional solitons propagating in a planar waveguide with power densities $L_e|E_{1,2}|^2$, L_e being the usual effective width along Y. In this case the linear confinement along Y prevents the transverse instability (a) from occurring; (c) $a_{1,2}=[\epsilon_{r1,2}(\rho,\phi)+i\epsilon_{i1,2}(\rho,\phi)]\cos(\Omega\tau)$ describing temporal instabilities of (2+1)-dimensional solitons in cylindrical coordinates (ρ,ϕ). Finally, note that for cw or quasi-cw soliton stripes in bulk, the transverse (a) and temporal (b) instabilities might in principle compete.

Substituting these expressions of $a_{1,2}$ in Eqs. (2), we obtain the following (4×4) real eigenvalue problem for the vector $\epsilon\equiv(\epsilon_r,\epsilon_i)^T$ with $\epsilon_{r,i}\equiv(\epsilon_{1r,i},\epsilon_{2r,i})^T$:

$$\begin{pmatrix}0 & -M^-\\ M^+ & 0\end{pmatrix}\epsilon-\lambda I_4\epsilon=0;M^\pm=\begin{pmatrix}L_1\pm x_2 & x_1\\ x_1 & L_2\end{pmatrix}, \tag{3}$$

where $I_4\equiv\mathrm{diag}(I_2,I_2)$, with $I_2\equiv\mathrm{diag}(1,\sigma)$, and $L_{1,2}$ are linear operators that depend on the specific problem (a)–(c). From Eq. (3), we obtain the decoupled problem $\lambda^2\epsilon_r=-I_2^{-2}M^-M^+\epsilon_r$ (and the adjoint problem for ϵ_i) that must be solved for unstable (with positive real part) eigenvalues λ. To this end, we first construct the whole families of soliton profiles $x_{1,2}=x_{1,2}(\rho;\alpha)$, solving the one-dimensional potential equations by means of the relaxation method [13]. Then, we solve Eq. (3) by means of the inverse iteration method [13] to find the spectral dependency of the gain $g=g(\Omega;\alpha)\equiv\mathrm{Re}[\lambda]$ associated with bounded eigenfunctions which fix the spatial shape of the growing perturbations. Below we report results obtained for $\sigma\approx 2$ (or $|\Delta k|/k_1\ll 1$).

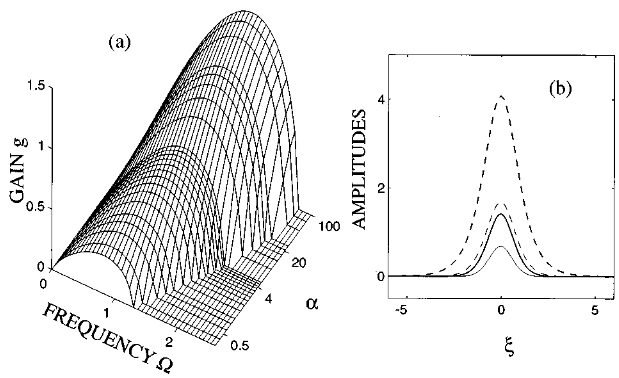

FIG. 1. (a) Spectral features of the transverse instability gain g for the stripe family parametrized by α (σ=2); (b) Eigenfunction ϵ_r (solid) and soliton (dashed) amplitude profiles for α=4 (δk=0). The thick and thin curves correspond to the fundamental and harmonic fields, respectively.

Let us consider first *the transverse stripe instability* [case (a)], for which we obtain $L_1\equiv\frac{1}{2}(\partial_\xi^2-r_1\Omega^2)-1$ and $L_2\equiv\frac{1}{2}(\partial_\xi^2-r_2\Omega^2)-\alpha$. The spectral gain $g(\Omega)$ is shown in Fig. 1(a) as a function of α. In Fig. 1(b) we show the eigenfunction profiles (their absolute vertical scale is arbitrary), superimposed to the soliton profiles for α=4. Although Eq. (3) admits both symmetric and antisymmetric eigensolutions $\epsilon(\xi)$, the transverse instability gain g *is always associated with the symmetric branch* (this conclusion is also consistent with our asymptotic analysis for small Ω).

Explicit results can be obtained when the soliton is available in closed form, i.e., $x_1/\sqrt{2}=x_2=(3/2)\mathrm{sech}^2\,(\xi/\sqrt{2})$ for $\alpha=1$. For $\beta_1=\beta_2$ $(L_1=L_2)$, the bifurcation point (i.e., $g=0$) in Eq. (3) yields the instability spectral range $0<\Omega<\Omega_c$ where the cut-off frequency $\Omega_c=\sqrt{5/2}$. Moreover, in the limit $\Omega\ll 1$, Eq. (3) is fulfilled by the asymptotic expression $g=a\Omega$ with $a=(r_1+2r_2)^{1/2}[2(1-2\sigma)^2I_s+(1+\sigma)^2]^{-1/2}$ with $I_s=\int_{-\infty}^{+\infty}f(x)\mathrm{sech}^2(x)\,dx\simeq-0.15$, $f(x)$ being a solution of the equation $f''-4f-6f\mathrm{sech}^2\,(\xi)=\mathrm{sech}^2\,(\xi)$. This result confirms that the symmetric branch requires $r_1+2r_2>0$ for $\sigma\approx 2$.

Once established that the soliton stripes are transversally unstable, a crucial issue is their long-range evolutions. Whenever the eigenfunction profiles follow those of the bell-shaped soliton, the dynamics of the instability process shows no significant changes along the trapping dimension and remains essentially one dimensional. Under these conditions it is reasonable to expect qualitative similarities (e.g., recurrence) with the evolution for modulational instability of plane waves. For instance, this occurs in cubic media [14], where recurrent or quasirecurrent plane-wave evolutions take place [15]. In SHG, however, the problem of long-range evolutions of plane waves is complicated by the large number of effective frequency modes, and hence *no similarities with solitons can be envisaged*. Here we investigate the nonlinear stage of soliton symmetry breaking by integrating numerically Eqs. (1) with the initial condition $u_{1,2}(X,Y,Z=0)=u_{1,2s}(X)+\overline{\epsilon}(X)\cos(\Omega_YY)$, where $\Omega_Y\equiv\sqrt{\mu}\Omega$ and the seed $\overline{\epsilon}(X)$ is a Gaussian-like perturbation with peak amplitude $\overline{\epsilon}(0)^2\approx 10^{-2}\,u_{1,2s}^2(0)$.

A typical result, obtained at phase matching $\delta k=0$ $(\alpha=4)$

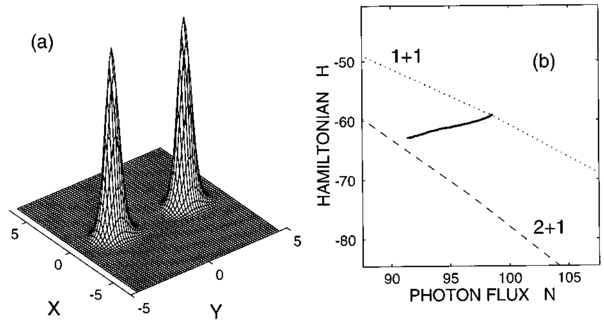

FIG. 2. Formation of a soliton lattice from an unstable stripe: (a) two-dimensional pattern formed at $Z=40$. Two periods $Y=2Y_p=4\pi/\Omega$ are shown. (b) Field evolution in the (N,H) plane. The existence curve of the stripes (1+1) and the cylindrical solitons (2+1) are also shown.

is shown in Fig. 2: the stripe breaks up into a periodical sequence of spots, forming a lattice of trapped waves, which are naturally expected to be (2+1)-dimensional solitons [Fig. 2(a)]. We verified this conjecture by drawing in Fig. 2(b) the evolutions of the contributions to the invariants, namely $N=\int_{-\infty}^{+\infty}\int_{-Y_p/2}^{Y_p/2} N_d \, dY dX$ and $H=\int_{-\infty}^{+\infty}\int_{-Y_p/2}^{Y_p/2} H_d \, dY dX$ related to any single spot within one period $Y_p=2\pi/\Omega_Y$. As the instability develops, the spots try to evolve toward the stable state of the system, radiating part of the energy along X (i.e., N and H decreases). This behavior is allowed whenever the existence curve of the stripe family (dotted curve) lies in the (N,H) plane above the one for cylindrical solitons (dashed curve), as shown in Fig. 2(b). This process is not strictly attractive, and the trajectory ends up in the proximity of the (2+1)-dimensional existence curve. Associated with the final excess flux N, the fields exhibit persistent oscillations as in the case of longitudinal instability [5]. In Fig. 3(a) we report the evolution of the three lowest-order transverse Fourier modes of the peak field $u_1(X=0,Y)$ (the field u_2 is not shown; it follows the dynamics of u_1, remaining phase-locked to it). As shown, after the transient which follows the amplification, the plane-wave and harmonic components stabilize into a regular amplitude oscillation. This implies also a a phase rotation which is conveniently described [15] by a limit cycle in the phase space ($\eta\cos\psi,\eta\sin\psi$), where η is the fraction of the first spatial Fourier harmonic and ψ $=2(\phi_{1,\Omega}-\phi_{1,0})$, $\phi_{1,n\Omega}$ being the phase of the nth Fourier mode [see Fig. 3(b)].

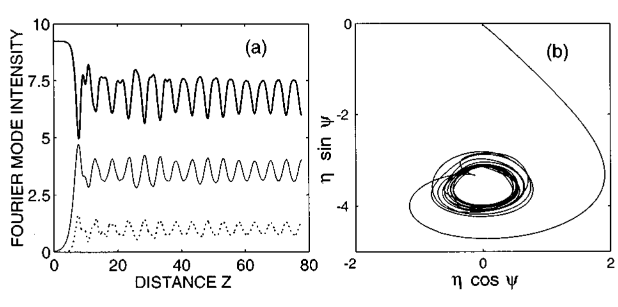

FIG. 3. Evolution of a soliton stripe at phase-mathing (α=4): (a) transverse Fourier modes of $u_1(X=0,Y,Z)$ versus distance Z: plane-wave component (Ω=0, thick solid curve); first harmonic (Ω, thin solid curve); second harmonic (2Ω, dotted curve); (b) phase-space representation.

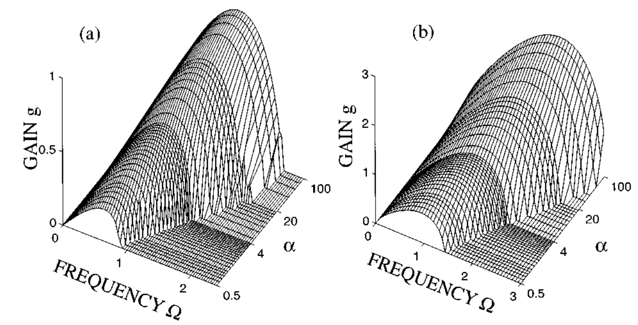

FIG. 4. Spectral features of the temporal instability gain g for the 2+1 soliton family versus α (σ=2): (a) normal dispersion regime ($\beta_1=\beta_2=1$); (b) anomalous dispersion regime ($\beta_1=\beta_2=-1$).

It can be shown that the problem of temporal instability [case (b)] can be treated in a similar way, with the formal substitution $r_{1,2}\rightarrow-\beta_{1,2}$ in the operators $L_{1,2}$ in Eqs. (3). Therefore, the temporal breakup in waveguides potentially lead to spatiotemporal trapping in the anomalous dispersion regime ($\beta_{1,2}<0$, no qualitative changes occur for $|\beta_2|\neq 1$), as discussed in detail for the transverse case (a). Conversely, in the normal dispersion regime ($\beta_{1,2}>0$) *no spatial analogy exists*. The unstable modes are antisymmetric and lead to spatiotemporal wave breaking with characteristic snakelike shapes [7], followed by the radiative decay of the soliton (for a detailed study see Ref. [16]). In this case, for $\alpha=1$, the bifurcation analysis gives the cut-off frequency $\Omega_c=\sqrt{3/2}$ for $\beta_1=\beta_2=1$. Moreover the asymptotic ($\Omega\ll 1$) gain is $g=a\Omega$ with $a=[3(2\beta_1+\beta_2)/5]^{1/2}[(1+\sigma)^2+\sigma(\sigma-2)^2I_a]^{-1/2}$, where $I_a=\int_{-\infty}^{+\infty}g(x)\tanh(x)\mathrm{sech}^2(x)\,dx\simeq-0.02$, $g(x)$ being the solution of the equation $g''-4g-12g\,\mathrm{sech}^2(\xi)=\tanh(\xi)\mathrm{sech}^2(\xi)$, which shows that the antisymmetric branch exists indeed for $2\beta_1+\beta_2>0$, i.e., in the normal dispersion regime (we leave for future analysis the case $\beta_1>0$, $\beta_2<0$, which is also physical).

Let us consider now *the instability of cylindrically symmetric solitons* [case (c)], described by Eqs. (3) with $L_1\equiv\frac{1}{2}(\partial_\rho^2+\rho^{-1}\partial_\rho-m^2\rho^{-2}+\beta_1\Omega^2)-1$ and $L_2\equiv\frac{1}{2}(\partial_\rho^2+\rho^{-1}\partial_\rho-m^2\rho^{-2}+\beta_2\Omega^2)-\alpha$, where we have assumed that the perturbed modes depend on the azimuthal phase ϕ as $\exp(im\phi)$, with m integer. A purely spatial instability cannot occur in this case because our analysis shows that Eqs. (3) *possess no unstable modes* for $\Omega\rightarrow 0$ (this is not necessarily the case for higher-order families of cylindrically symmetric solitons with nodes). Conversely, the whole soliton family is unstable with respect to temporal wave breaking ($\Omega\neq 0$) both in the normal ($\beta_{1,2}>0$) and anomalous ($\beta_{1,2}<0$) dispersion regimes. The spectral gain $g(\Omega;\alpha)$ calculated numerically (no explicit cylindrical solutions are known) is shown in Fig. 4. As shown, the instability is stronger and involves higher frequencies with anomalous dispersion [Fig. 4(b)]. However, the two dispersive regimes exhibit qualitatively different features related to the radial (shown in Fig. 5) and azimuthal symmetry of the unstable eigenfunctions. With normal dispersion the most unstable eigenfunctions have a doughnut radial profile and correspond to $m=1$; see

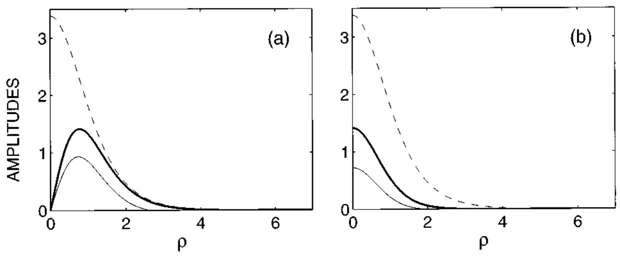

FIG. 5. Radial profiles of the unstable modes ϵ_{r1} (thick solid curve), and ϵ_{r2} (thin solid curve) for $\alpha=1$, $\sigma=2$, (a) $\beta_1=\beta_2=1$; (b) $\beta_1=\beta_2=-1$. For comparison we show the corresponding soliton profile (u_1 field, dashed curve).

Fig. 5(a). As a consequence the temporal breaking is expected to be accompanied by the emission of ring-shaped beams which can further induce spatial wave breaking due to their azimuthal phase dependence, leading to intricate spatiotemporal patterns. Vice versa, in the anomalous dispersion regime, the unstable modes exhibit no azimuthal dependence $(m=0)$, and have bell-shaped radial profiles; see Fig. 5(b). Therefore, this case is reminiscent of the transverse stripe instability discussed above. It is reasonable to expect that the long-range evolution leads to a final oscillatory state around a lattice of two-color optical bullets [(3+1)-dimensional solitons], a phenomenon that will be explored in the future.

Finally, let us delineate our expectation for real experiments made with beams of constant physical width [4,11], say x_s (i.e., $X=x_s/r_0=1$). From the expression of the real-world soliton width $x_s=r_0\xi_s/\sqrt{\mu}$ ($\xi_s=\xi_s(\alpha)$ being the normalized width obtained from the potential equations for the whole family), we obtain the additional constraint $\mu=\xi_s^2$. Hence, the one-parameter family can be spanned at constant beam width r_0 ($\sigma\simeq 2$), by changing the physical mismatch according to the law $\Delta k=\mu(2-\alpha/\sigma)/z_d=(4-\alpha)\xi_s^2(\alpha)/(2k_1r_0^2)$. The instability can be observed whenever the sample is comparable or longer than the physical gain length $z_g\equiv 10z_d/(g\mu)=20k_1r_0^2/(g\xi_s^2)$. For instance, a full width at half maximum (FWHM) physical width $r_0=10$ μm, and $k_1=10^5$ cm^{-1} yield for $\alpha=1$ (sech^2 soliton with FWHM width $\xi_s=1.7$), $z_g\simeq 1$ cm, and a physical lattice spacing $y_p=2\pi r_0/(\Omega\xi_s)\simeq 40$ μm for $\Omega=1$, (under quasi-plane-wave excitation [11], the beam must be much wider than y_p). The required peak intensity is $|E_1|^2=|E_2|^2/2=|u_{1s}|^2/(2\chi^2 z_d^2)\simeq 1$ GW/cm^2 for $\chi=5\times 10^{-4}$ $W^{-1/2}$ ($d_{eff}=6$ pm/V in $KTiPO_4$ [4,11]).

In summary, we have shown that parametric solitons undergo symmetry-breaking instabilities. The transverse or temporal breakup of one-dimensional solitons can lead to oscillations around a lattice of higher-dimensional solitons. The loss of symmetry for cylindrically symmetric solitons can occur only through temporal break-up, associated with the growth of either bell-shaped modes, or nonazimuthally symmetric doughnut modes.

We thank D. E. Pelinovsky, G. Assanto, and G. I. Stegeman for useful discussions. A.V.B. acknowledges a financial support of the Australian Research Council.

[1] R. Y. Chiao, E. Germire, and G. Townes, Phys. Rev. Lett. **13**, 478 (1964); **14**, 1056 (1965).
[2] Y. N. Karamzin and A. P. Sukhorukov, Pis'ma Zh. Eksp. Teor. Fiz. **20**, 734 (1974) [JETP Lett. **20**, 339 (1974)]; Zh. Eksp. Teor. Fiz. **68**, 834 (1975) [Sov. Phys. JETP **41**, 414 (1976)].
[3] A. V. Buryak and Yu. S. Kivshar, Opt. Lett. **19**, 1612 (1994); Phys. Lett. A **197**, 407 (1995); L. Torner, D. Mazilu, and D. Mihalache, Phys. Rev. Lett. **77**, 2455 (1996); H. He, W. J. Werner, and P. D. Drummond, Phys. Rev. E **54**, 896 (1996); G. I. Stegeman, D. J. Hagan, and L. Torner, Opt. Quantum Electron. **28**, 1691 (1997).
[4] W. E. Torruellas *et al.*, Phys. Rev. Lett. **74**, 5036 (1995); R. Schiek, Y. Baek, and G. I. Stegeman, Phys. Rev. E **53**, 1138 (1996).
[5] D. E. Pelinovsky, A. V. Buryak, and Yu. S. Kivshar, Phys. Rev. Lett. **75**, 591 (1995); A. V. Buryak, Yu. S. Kivshar, and S. Trillo, *ibid.* **77**, 5210 (1996).
[6] S. Trillo and P. Ferro, Opt. Lett. **20**, 438 (1995).
[7] E. A. Kuznetsov, A. M. Rubenchik, and V. E. Zakharov, Phys. Rep. **142**, 103 (1986).
[8] Transverse soliton break-up is observed in photorefractives: A. V. Mamaev, M. Saffman, and A. A. Zozulya, Europhys. Lett. **35**, 25 (1996). To our knowledge, the snake-instability of bright solitons was not demonstrated.
[9] D. E. Pelinovsky, V. V. Afanasjev, and Yu. S. Kivshar, Phys. Rev. E **53**, 1940 (1996).
[10] A. A. Kanashov and A. M. Rubenchik, Physica D **4**, 122 (1981); L. Berge, V. K. Mezentsev, J. J. Rasmussen, and J. Wyller, Phys. Rev. A **52**, R28 (1995); S. K. Turitsyn, Pis'ma Zh. Eksp. Teor. Fiz. **61**, 458 (1995) [JETP Lett. **61**, 469 (1995)].
[11] R. A. Fuerst *et al.*, Phys. Rev. Lett. **78**, 2756 (1997).
[12] K. Dholakia *et al.*, Phys. Rev. E **54**, R3742 (1996).
[13] W. H. Press *et al.*, *Numerical Recipes* (Cambridge University Press, Cambridge, 1990), p. 377.
[14] J. M. Soto-Crespo, E. M. Wright, and N. N. Akhmediev, Phys. Rev. A **45**, 3168 (1992).
[15] M. J. Ablowitz and P. A. Clarkson, *Solitons, Nonlinear Evolution Equations and Inverse Scattering* (Cambridge University, Cambridge, 1991), pp. 127–152; S. Trillo and S. Wabnitz, Opt. Lett. **16**, 986 (1991); H. C. Yuen and W. E. Ferguson, Phys. Fluids **21**, 2116 (1978).
[16] A. De Rossi, S. Trillo, A. V. Buryak, and Yu. S. Kivshar, Opt. Lett. **22**, 868 (1997).